

DAS35

# Yielding and strain localization effects in gum metal - a unique Ti alloy - investigated by digital image correlation and infrared thermography

Elżbieta A. Pieczyska<sup>a,\*</sup>, Karol Golański<sup>a</sup>, Michał Maj<sup>a</sup>, Maria Staszczak<sup>a</sup>,  
Zbigniew Kowalewski<sup>a</sup>, Tadahiko Furuta<sup>b</sup>, Shigeru Kuramoto

<sup>a</sup> *Institute of Fundamental Technological Research, PAS, Pawińskiego 5 B, 02-106 Warsaw, Poland*

<sup>b</sup> *Toyota Central Research & Development Labs, Nagakute, Aichi, 480-1192, Japan*

<sup>c</sup> *Ibaraki University; 4-12-1, Nakanarusawa, Hitachi, 316-8511, Japan*

---

## Abstract

The research concerns investigation of yielding and developing of the strain localization in new  $\beta$ -Ti alloy characterized by unique elastic-plastic properties, named Gum Metal. The alloy was subjected to tension on testing machine at three various strain rates up to rupture. Digital image correlation and infrared thermography were applied to analyze the experimental results. Strain distributions were determined on the basis of digital image correlation algorithm. The related temperature variations were found in contactless manner using infrared thermography. Mechanical and the corresponding thermal data were used to study the Gum Metal large nonlinear reversible deformation and localization effects.

© 2019 Elsevier Ltd. All rights reserved.

Selection and peer-review under responsibility of 35th Danubia Adria Symposium on Advances in Experimental Mechanics.

*Keywords:* Gum Metal; tension; large nonlinear elastic deformation; thermomechanical couplings; temperature change; digital image correlation

---

## 1. Experimental procedure

The experimental setup [Fig. 1] consists of MTS 858 TM and two cameras working in two different spectral ranges: visible (0.3-1  $\mu\text{m}$ ) Manta G-125B and IR (3-5  $\mu\text{m}$ ) ThermaCam Phoenix. Dog bone sample with sizes of

---

\* Corresponding author. Tel.: +48 22 8261281/369; fax: +48 22 8267380.

E-mail address: [epiecz@ippt.pan.pl](mailto:epiecz@ippt.pan.pl)

Nomenclature	
DIC	Digital Image Correlation
IRT	Infrared Thermography
TM	Testing Machine

100 mm x 8 mm x 0.5 mm were used, gauge part 7 mm x 4 mm; length of virtual extensometer for DIC - 7 mm. The surface of the samples were coated with sooth and the emissivity was assumed to be 0.95. Details including numerical procedures of the DIC algorithm are presented in [1]. More experimental results on investigation of effects of thermomechanical couplings in Gum Metal under tensile loading are presented in [2-4].

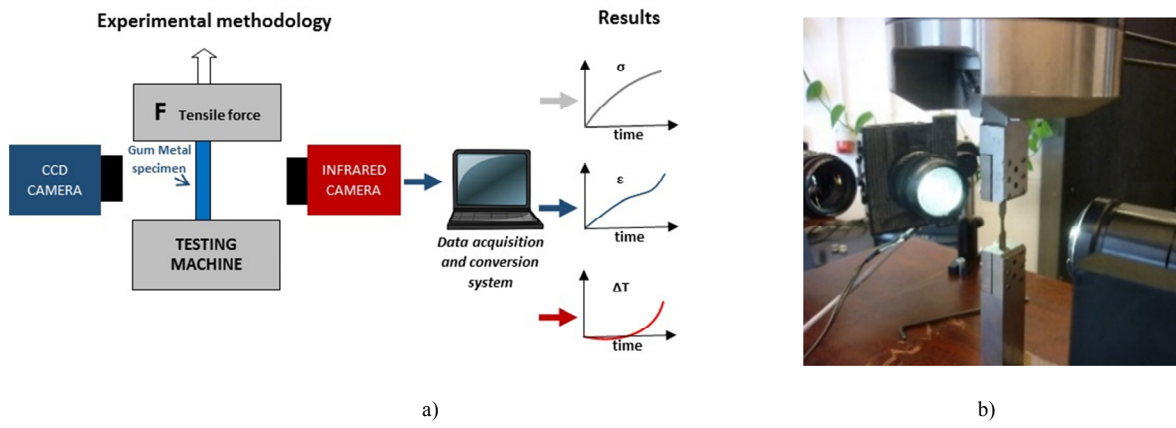


Fig. 1. a) Scheme and b) photograph of experimental set-up used for investigation of deformation and thermal fields in Gum Metal

## 2. Gum Metal yielding and strain localization - mechanical and thermal results

The stress  $\sigma$  and mean temperature changes ( $\Delta T_{mean}$ ) of the Gum Metal specimen vs. strain, obtained during tension at strain rate of  $10^{-2} s^{-1}$  up to strain 0.025, is shown in Fig. 2.

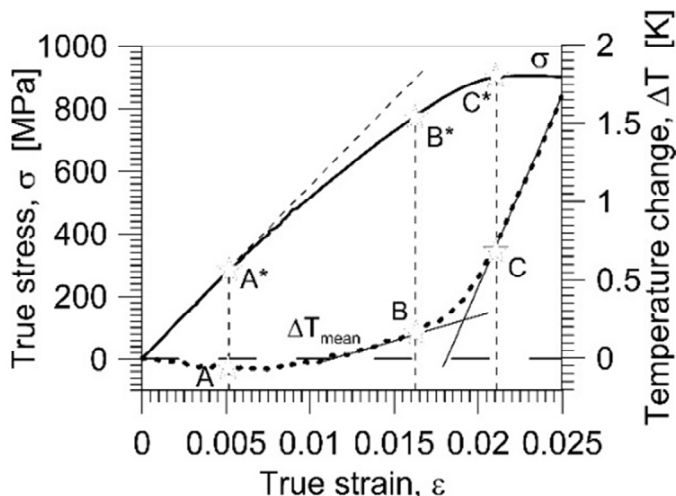


Fig. 2. Stress  $\sigma$  and temperature change ( $\Delta T_{mean}$ ) vs. strain  $\epsilon$  obtained for Gum Metals tension at strain rate of  $10^{-2} s^{-1}$  up to 0.025

The elastic limit, corresponding to maximal drop in the specimen temperature, and limit of mechanically reversible deformation, found in subsequent cyclic loading [2], are marked by  $A^*$  and  $B^*$ , respectively (Fig. 2).

Increase in the specimen temperature (after its drop due to thermoelastic effect) started from point A revealed dissipative character of the process, probably caused by stress-induced phase transformation of martensite-like orthorhombic  $\alpha''$  nanodomains [5,6]. Furthermore, small increase in the temperature in this range can be a sign that the transition takes place in small volume of the alloy, what is consistent with the results of microstructure analysis [6]. From the points B and C the slope of dependence  $\Delta T$  vs.  $\varepsilon$  increases demonstrating that the deformation is irreversible from both thermodynamic and mechanical points of view at this stage. The growth in temperature demonstrates exothermal nature of the governing deformation occurring in Gum Metal, also within the reversible strain range.

Stress vs. strain curves derived by DIC for the Gum Metal tension at three various strain rates till rupture, completed by the related temperature changes are presented in Figs 3 a, b and c. IR thermograms (left) and corresponding DIC distributions of the  $E_{yy}$  strain component (right) for the strain 0.07 (vertical dashed line in diagrams) are shown. Two kinds of the temperature of the gauge part of the specimen are analyzed: mean  $\Delta T_{mean}$  and maximal  $\Delta T_{max}$ .

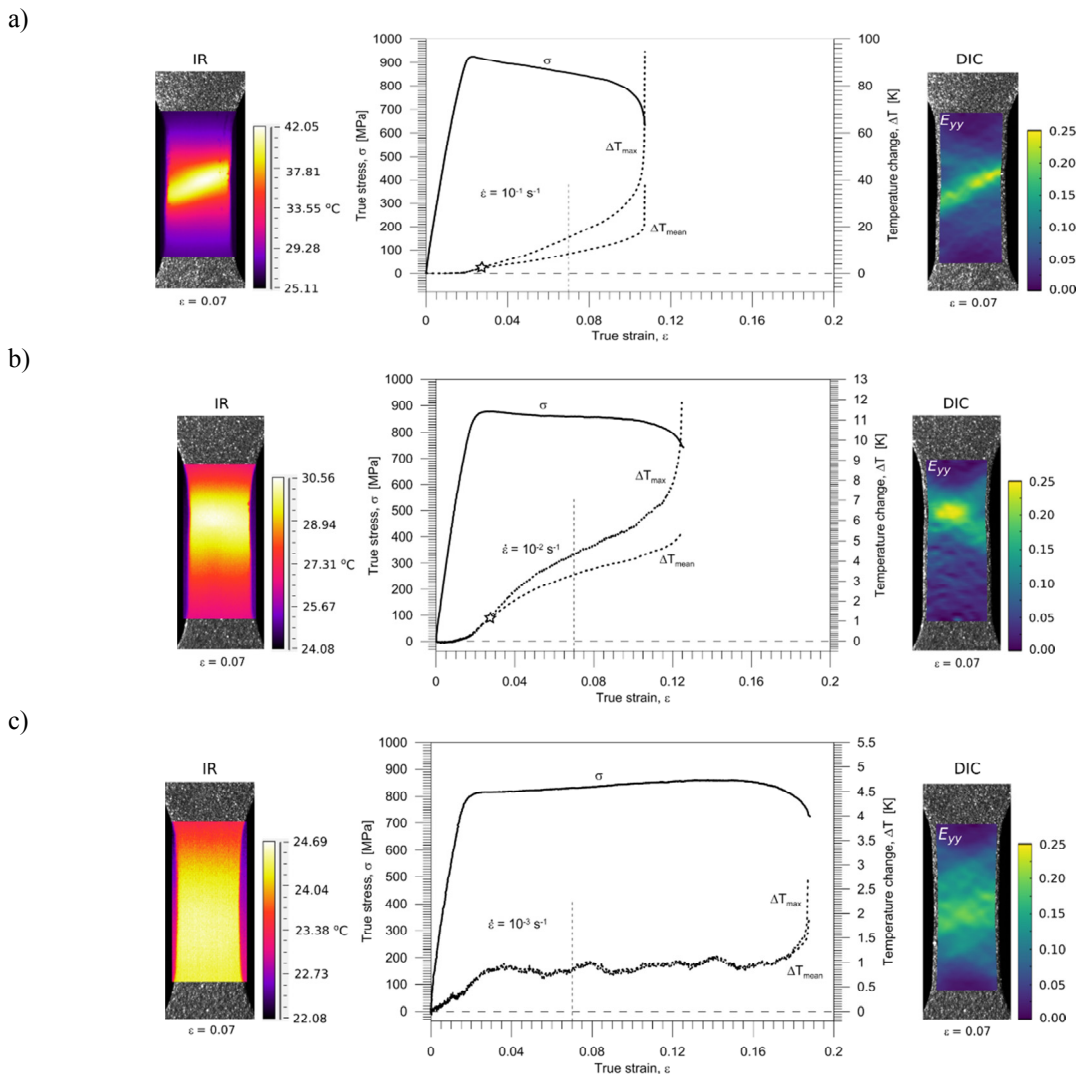


Fig. 3. Stress, maximal  $\Delta T_{max}$  and mean  $\Delta T_{mean}$  temperature change vs. strain for strain rates: (a)  $10^{-1} \text{ s}^{-1}$ , (b)  $10^{-2} \text{ s}^{-1}$ , (c)  $10^{-3} \text{ s}^{-1}$ . In addition, thermograms (left) and corresponding  $E_{yy}$  strain component distributions (right) obtained for the strain value 0.07 (vertical dashed line) are shown

In the initial strain range the  $\Delta T_{max}$  and  $\Delta T_{mean}$  curves are overlapping; at the higher strains a gradually increasing discrepancy between the curves is observed (Fig. 3). The point of the discrepancy (marked by a star) is an indicator of the onset of localization of the plastic strain. At the lower strain rate equal to  $10^{-3}\text{s}^{-1}$  no discrepancy is seen between the maximal and average temperature curves, yet the obtained non-uniform strain distribution demonstrates also the strain localization.

### 3. Discussion

Comparison of the strain values at which the strain localization initiates as well as estimated values of the maximal stress, strain and the maximal and average temperature changes obtained for the Gum Metal specimen rupture at three various strain rates is presented in Table 1.

Table 1 Comparison of mechanical and thermal parameters obtained during Gum Metal tensile loading to rupture at three strain rates

Strain rate	Strain value at the point where localization starts	Maximal stress value	Maximal strain value	Average temperature change at rupture	Maximal temperature change at rupture
$10^{-3}\text{s}^{-1}$	no	861 MPa	0.188	1.88 K	5.4 K
$10^{-2}\text{s}^{-1}$	0.0224	878 MPa	0.124	5.47 K	12 K
$10^{-1}\text{s}^{-1}$	0.0208	925 MPa	0.107	38.68 K	94.6 K

It should be noticed in Fig. 3 a, b that from the stage where the strain localization starts, the macroscopically observed strain softening takes place. For the strain rate  $10^{-1}\text{s}^{-1}$  the plastic strain localization occurs immediately beyond the limit of the mechanically reversible deformation (Fig. 3a). At the strain rate of  $10^{-3}\text{s}^{-1}$ , far from adiabatic conditions, no discrepancy is seen between the maximal and average temperatures. Nevertheless, the obtained non-uniform strain distribution demonstrates the strain localization for the all strain rates applied.

### 4. Concluding remarks

Large limit of the Gum Metal reversible nonlinear deformation, underlined as the unique alloy "super property", originates from mechanisms of dissipative nature; exothermic stress-induced transition of  $\alpha''$  nanodomains.

The point of the discrepancy, obtained between the maximal  $\Delta T_{max}$  and mean  $\Delta T_{mean}$  temperature vs. strain curves, indicates on the onset of the Gum Metal plastic strain localization.

Both strain and temperature distributions demonstrate that at the higher strain rates the strain localization starts nucleating just after the Gum Metal yield limit.

### Acknowledgements

The research was supported by the National Science Centre, Poland; under Projects: No. 2014/13/B/ST8/04280 and No. 2016/23/N/ST8/03688.

### References

- [1] M. Nowak, M. Maj M., Arch. Civil Mech. Eng. 18 (2018) 630-644.
- [2] E.A. Pieczyska, M. Maj, K. Golański, M. Staszczak, T. Furuta, S. Kuramoto, Materials 11 (2018) 1-13.
- [3] K.M. Golański, E.A. Pieczyska, M. Staszczak, M. Maj, T. Furuta, S. Kuramoto, QIRT J. 14 (2017) 226-233.
- [4] E.A. Pieczyska, M. Maj, T. Furuta, S. Kuramoto (2016) Gum Metal– unique properties and results of initial investigation of a new titanium alloy – extended paper. In: Kleiber M et al. (ed) Advances in Mechanics: Theoretical, Computational and Interdisciplinary, CRC Press/Balkema, Taylor & Francis, London, 469-472.
- [5] S. Kuramoto, T. Furuta, J. Hwang, K. Nishino, T. Saito, Mater. Sci. Eng. A. 442 (2006) 454-457.
- [6] L.S. Wei, H.Y. Kim, T. Koyano, S. Miyazaki, Scr. Mater. 12 (2016) 55–58.